The environmental carcinogen 3-nitrobenzanthrone and its main metabolite 3-aminobenzanthrone enhance formation of reactive oxygen intermediates in human A549 lung epithelial cells

Tanja Hansen[a]*, Albrecht Seidel[b] and Jürgen Borlak[a]

[a]Fraunhofer Institute of Toxicology and Experimental Medicine, Nikolai-Fuchs-Str. 1, 30625 Hannover, Germany,

[b]Biochemical Institute for Environmental Carcinogens, Prof. Dr. Gernot Grimmer Foundation, Lurup 4, 22927 Grosshansdorf, Germany

*Address correspondence to:
Dr. Tanja Hansen
Fraunhofer Institute of Toxicology and Experimental Medicine
Nikolai-Fuchs-Str. 1
30625 Hannover
Germany

Phone: +49 511 5350 226
Fax: +49 511 5350 155
E-mail: tanja.hansen@item.fraunhofer.de

Abbreviations

AEC	Alveolar epithelial cell
3-NBA	3-nitrobenzanthrone
3-ABA	3-aminobenzanthrone
ROS	reactive oxygen species
TTFA	thenoyltrifluoroacetone
AA	antimycin A
PAH	polycyclic aromatic hydrocarbons
NQO1	NAD(P)H:quinone oxidoreductase
CYP	cytochrome P450
NAT	*N,O*-acetyltransferase
SULT	sulfotransferase
EROD	ethoxyresorufin-*O*-deethylase
DMEM	Dulbecco's Modified Eagle Medium
DCFH-DA	2',7'-Dichlorofluorescin-diacetate
DCF	2',7'-dichlorofluorescein
BP	benzo[*a*]pyrene
DFO	desferrioxamine mesylate
DEP	diesel exhaust particles

Abstract

The environmental contaminant 3-nitrobenzanthrone (3-NBA) is highly mutagenic and a suspected human carcinogen. We aimed to evaluate whether 3-NBA is able to deregulate critical steps in cell cycle control and apoptosis in human lung epithelial A549 cells. Increased intracellular Ca^{2+} and caspase activities, were detected upon 3-NBA exposure. As shown by cell cycle analysis, an increased number of S-phase cells was observed after 24 h of treatment with 3-NBA. Furthermore, 3-NBA was shown to inhibit cell proliferation when added to subconfluent cell cultures. The main metabolite of 3-NBA, 3-ABA, induced statistically significant increases in tail moment as judged by alkaline comet assay. The potential of 3-NBA and 3-ABA to enhance the production of reactive oxygen species (ROS) was demonstrated by flow cytometry using 2',7'-Dichlorofluorescin-diacetate (DCFH-DA). The enzyme inhibitors allopurinol, dicumarol, resveratrol and SKF 525A were used to assess the impact of metabolic conversion on 3-NBA-mediated ROS production. Resveratrol decreased dichlorofluorescein (DCF) fluorescence by 50 %, suggesting a role for CYP1A1 in 3-NBA-mediated ROS production. Mitochondrial ROS production was significantly attenuated (20 % reduction) by addition of rotenone (complex I inhibition) and thenoyltrifluoroacetone (TTFA, complex II inhibition). Taken together, the results of the present study provide evidence for a genotoxic potential of 3-ABA in human epithelial lung cells. Moreover, both compounds lead to increased intracellular ROS and create an environment favorable to DNA damage and the promotion of cancer.

Keywords: 3-nitrobenzanthrone, 3-aminobenzanthrone, diesel exhaust, reactive oxygen species, DNA damage, cell cycle

Introduction

Air pollution by emission from diesel and gasoline engines is an important risk factor for human health in industrialized countries. Epidemiologic research suggested that exposure to air pollution plays a causative role in lung cancer (Hemminki and Pershagen, 1994; Silverman, 1998; Boffetta et al., 2001). Furthermore, diesel exhaust has been classified by the International Agency for Research on Cancer as probably carcinogenic to humans (IARC, 1989).

Nitrated PAH are abundant in diesel exhaust and airborne particulate matters (Enya and Suzuki, 1997). They are formed during incomplete combustion of fossil fuels as well as by reaction of parent hydrocarbons with nitrogen oxides, UV light and ozone in ambient air (Aktinson and Arey, 1994). The carcinogenicity and mutagenicity of nitrated PAH is well documented (Rosenkranz, 1996). Among this class of compounds, 3-nitrobenzanthrone (3-NBA, 3-nitro-7*H*-benz[*de*]anthracene-7-one) is one of the most potent mutagens in the AMES *Salmonella typhimurium* (TA98, TA100, YG1024, YG1029) assay (Enya and Suzuki, 1997; Watanabe et al., 2005). 3-NBAs ability to induce lung tumor formation in rats after intratracheal administration has been reported by Nagy et al., 2005. In the latter study, squamous cell carcinomas were found in the high dose group (22 mg/kg total dose) after 7-9 month and in the low dose group (15 mg/kg total dose) after 10-12 months, respectively. The ability of 3-NBA to cause DNA adduct formation has been shown *in vitro* after activation by xanthine oxidase and by rat liver S9 (Bieler et al., 1999), in primary rat alveolar type II cell cultures (Borlak et al., 2000), in human hepatoma cells (Kawanishi et al., 2000) and *in vivo* in rats (Nagy et al., 2005; Arlt et al., 2001, 2002, 2003a, 2003b). 3-NBA has been detected in surface soil at 144-1158 pg/g and in rain water at 0.07-2.6 ng/l, demonstrating ubiquitous

contamination with this carcinogen (Murahashi et al., 2003; Watanabe et al., 2003). The main metabolite of 3-NBA, 3-aminobenzanthrone (3-ABA) has been detected in urine of mining workers occupationally exposed to diesel exhaust in similar concentrations (1 - 143 ng/24h urine) as 1-aminopyrene, a metabolite of the widely spread environmental contaminant 1-nitropyrene (Seidel et al., 2002). This finding shows, that occupational human exposure to 3-NBA can be significant. Data on plasma concentrations of 3-NBA or 3-ABA in occupationally exposed humans are not available so far. Similarly, it is not known, which concentrations are reached in the target cells of the respiratory tract, namely bronchial and alveolar epithelial cells. However, DNA adducts may be used as biomarkers for occupational and environmental exposure. In a recent study, Nagy et al. (2006) investigated the time course of DNA adduct formation in F344 rats after oral administration of 3-NBA. It was shown in this study, that maximum adduct levels were reached 10 days after administration with highest levels being detected in the lung kidney and stomach. The authors conclude from these findings that 3-NBA might be stored in tissues and later become bioavailable resulting in higher adduct levels in target tissues. It can thus not be ruled out, that 3-NBA or its main metabolite 3-ABA have the potential to accumulate in lung epithelial cells.

Nitroarenes require metabolic activation to electrophilic metabolites to become genotoxic carcinogens. Activation of nitroarenes can occur through nitroreduction, catalyzed by xanthine oxidase, NAD(P)H:quinone oxidoreductase (NQO1) and aldehyde oxidase, or through oxidative metabolism, which is thought to be mediated by cytochrome P450s. In a recent study, we demonstrated metabolic activation and DNA binding of 3-NBA in alveolar epithelial cells, which are thought to be the target cells of 3-NBA-induced toxicity upon exposure via the respiratory tract. Inhibition experiments with allopurinol provided evidence that the cytosolic enzyme xanthine oxidase contributes substantially to the biotransformation of 3-NBA in this particular cell type (Borlak et al., 2000).

Arlt and co-workers investigated the role of human *N,O*-acetyltransferases and sulfotransferases in the metabolic activation of 3-NBA (Arlt et al., 2002). Using V79 cells expressing recombinant human NAT1, NAT2 or SULT1A1, it was shown that NAT1 and to a lesser extent NAT2 and SULT1A1 contribute to the genotoxic potential of 3-NBA to form DNA adducts. Bacterial mutagenicity assays with *Salmonella typhimurium* strains expressing recombinant human NATs revealed 3.8-fold and 16.8-fold higher mutagenic potentials of 3-NBA in Salmonella strains expressing NAT1 and NAT2, respectively, when compared with an acetyltransferase-deficient strain. In a recent study, it was shown that NQO1 is the major enzyme responsible for the reductive metabolism of 3-NBA in human hepatic cytosols and that conjugation of the reductive metabolites occurs mainly via NATs and SULTs (Arlt et al., 2005). The main metabolite of 3-NBA, 3-ABA, is not only a suitable biomarker for occupational exposure to 3-NBA but also a genotoxic carcinogen by itself, capable of forming DNA adducts. It has been shown that metabolic activation of 3-ABA to DNA-binding species can be catalyzed by CYP1A1, CYP1A2 and different peroxidases (Arlt et al., 2004 and 2006).

Several enzymes involved in the metabolic activation of 3-NBA are important for the regulation of the intracellular redox state. For instance, NQO1 (Vasiliou et al., 2006) catalyzes the two-electron reduction of quinones to hydroquinones, thereby preventing the one-electron reduction of quinones by cytochrome P450 and other flavoproteins that would lead to generation of superoxide. Xanthine oxidase is able to produce reactive oxygen species (ROS) by reduction of molecular oxygen to superoxide radical and hydrogen peroxide. It is thus conceivable that metabolic conversion of 3-NBA or 3-ABA in alveolar epithelial cells might be associated with increased ROS production. ROS are important signaling molecules regulating protein phosphorylation, gene expression, transcription factor activation, DNA synthesis and

cell proliferation (Hoidal, 2001; Shackelford et al., 2000). As a result, ROS play an important role in cancer promotion.

It was the aim of the present study to investigate whether the metabolic activation of 3-NBA or 3-ABA by human epithelial lung cells leads to increased production of ROS. Enzyme inhibition studies with allopurinol, dicumarol, SKF525A and resveratrol were performed in order to identify the enzymes responsible for 3-NBA- or 3-ABA-mediated ROS production. Furthermore, sources of mitochondrial ROS production were investigated as well as the effects of 3-NBA on cell cycle control and apoptosis.

We decided to use an immortalized cell line as a model of the human lung epithelium because it is possible to study many different treatment conditions in such an in vitro system in order to gain insight in the underlying mechanisms. Due to animal welfare aspects, it is not possible to perform all mechanistic studies with experimental animals, even though *in vivo* animal studies are most probably more relevant for the human in vivo situation than cell culture models. Primary cells might be a good alternative provided that the model is standardized and well characterized with respect to cellular differentiation during culture time. However, a great disadvantage is the limitet availability of human tissue or the poor cell yield obtainable from laboratory animals, which make primary cells insufficient to do mechanistic studies with a large number of treatment conditions.The A549 cell line is currently one of the best characterized cell lines of human pulmonary origin. The morphology an basic cellular functions, such as surfactant synthesis, oxidative metabolism and transport properties are consistent with those of alveolar epithelial type II cells (Foster et al., 1998), even though A549 cells are cancer cells. The expression and inducibility of cytochrome P450s in A549 cells has been shown previously (Hukkanen et al., 2000; Castell et al., 2005). Furthermore, A549 cells have been used as a

model for alveolar type II cells to study ROS generation, cell cycle control and apoptosis (Ovrevik et al., 2006; Zhu and Gooderham, 2006; Chien et al., 2006) and it has been shown in these studies, that important molecular signalling pathways (e.g. MAPK, NF-κB, PI3K/Akt, WAF1/p21, KIP1/p27) are expressed and well characterized in this cell line. However, it should be considered that A549 cells are a transformed cell line derived from a lung tumor. Abnormal expression of cell cycle regulatory molecules may cause alteration in cell cycle control. The majority of tumor cells have lost the ability to to stop at predetermined points of the cell cycle, prevalently due to the inactivation of critical CDK inhibitors or to overexpression of cyclins. It is thus conceivable, that the results obtained with A549 cells may be different from normal lung epithelial cells, when effects on cell cycle regulation are studied. For instance, Khan et al investigated the effects of a potential chemopreventive agent on growth inhibition in A549 cells and normal human bronchial epithelial cells (NHBE) and it was shown that A549 cells were much more sensitive to the growth inhibitory effects than the normal cell line. Nevertheless, as many important pathways are known to be expressed in this cell line, we judged A549 a suitable model for this study to generate hypotheses on 3-NBAs mechanism of action. However, the relevance for the human *in vivo* situation will have to be confirmed by *in vivo* studies.

Methods

Chemicals and reagents

3-NBA was synthesized according to the method described in Houben-Weyl (Müller and Bayer, 1979). Briefly, to a suspension of powdered benzanthrone (50 g) in nitro benzene (425 g) was added 87% nitric acid (33 g) within 1 h at room temperature. The mixture is subsequently heated at 50°C for 3 h and than allowed to cool to room temperature. Ethanol (500 mL) is added to the mixture under stirring and the resulting crude product (41 g) is filtered and washed with ethanol. Pure 3-NBA is obtained by two recrystallizations from acetic acid; yellow needles, mp 248°C.

3-ABA was synthesized according to method published in Houben-Weyl (Müller and Bayer, 1979) with slight modifications. Briefly, 3-NBA (19.8 g) was mixed with a 15% aqueous solution of sodium sulfite (200 mL) and stirred for 0.5 h. The mixture was heated under reflux for 1 h and then filtered, washed with hot water and dried. The crude product was recrystallized from chlorobenzene to afford 15.6 g 3-ABA (88% yield); mp 239°C, UV λ_{max} (ε [cm^2mmol^{-1}]) 206.0 (43,400) 282.0 (28,300) 517.0 (9,100), NMR (Bruker AV400, 400 MHz in DMSO-d_6) δ (ppm) 8.73 (dd, H-6, J=8,2 Hz, J=1.1 Hz) 8.66 (dd, H-7, J=7.4 Hz, J=1.1 Hz) 8.47 (d, H-1, J=8.4 Hz) 8.36 (d, H-4, J=8.2 Hz) 8.27 (dd, H-10, J=7.9 Hz, J=1.3 Hz) 7.76 (t, H-5) 7.72 (m, H-8) 7.41 (m, H-9) 6.90 (s, -NH_2) 6.88 (d, H-2); mass spectrum, m/z = 245.9 (100, M^+) 217 (M^+-CO); The purity of 3-ABA was proven by HPLC and no impurities were found using a Bakerbond PAH 16-plus column under isocratic conditions with a mixture of H_2O and CH_3OH (50 : 50, v/v) as eluent.

Reagents and fluorescent dyes were purchased from the following sources: 2',7'-Dichlorofluorescin-diacetate (DCFH-DA) was from Calbiochem (Schwalbach, Germany).

Fluo-3 and $(Asp)_2$-rhodamine 110 were obtained from Molecular Probes Inc. (Eugene, USA). The enzyme inhibitors allopurinol, dicumarol, resveratrol and SKF 525A as well as the iron chelator desferrioxamine mesylate (DFO), 7-ethoxyresorufin, resorufin, rotenone, thenoyl-trifluoroacetone (TTFA) and antimycin A (AA) were from Sigma (Taufkirchen, Germany). Cell cycle analysis was done using a commercially available kit (CycleTEST™, Becton Dickinson).

HPLC analysis of 3-NBA and its metabolites

3-NBA and its metabolites were analyzed in cell culture medium only and not in the intracellular fraction. The HPLC method has been described previously (Borlak et al., 2000).

Dose rationale

In a previous study (Borlak et al., 2000), we investigated metabolism and DNA-binding of 3-NBA in primary rat alveolar epithelial cells (AECs). The relatively high dose (6 µmol/L) was necessary in this study to yield sufficient material for the analysis of DNA-adducts and the HPLC analysis af 3-NBA and its metabolites. In order to compare metabolism and effects of 3-NBA between primary rat AECs and human lung epithelial A549 cells, the same dose level was chosen in the current study. It was shown to be non-cytotoxic to primary rat AECs and confluent A549 cells. With intend to show that lower concentrations, that might be more relevant for the in vivo situation, produce similar effects, some experiments were additionally performed with 100 nmol/L 3-NBA.

Cell culture and experimental design

The human lung adenocarcinoma cell line A549 was obtained from the German Collection of Microorganisms and Cell Cultures (Braunschweig, Germany). A549 cells were cultured in Dulbecco's Modified Eagle Medium (DMEM, Biochrom, Berlin, Germany) supplemented with 10 % fetal bovine serum (PAA Laboratories, Cölbe, Germany). Experiments were conducted

with subconfluent cultures. A549 cells were treated with 3-nitrobenzanthrone (3-NBA) or 3-aminobenzanthrone (3-ABA) for different time intervals and at different concentrations as indicated in the figure legends. The enzyme inhibitors allopurinol, dicumarol, resveratrol and SKF 525A (10 µmol/L each) were used in combination with 3-NBA to assess the impact of metabolic conversion on 3-NBA-mediated ROS production. The iron chelator desferrioxamine mesylate (DFO) was added at 10 µmol/L to assess the impact of Fenton-type reactions on the production of hydrogen peroxide. DFO and the enzyme inhibitors were added to the cell cultures 3 hours prior to treatment with 3-NBA or 3-ABA. The culture medium was removed after the preincubation period and fresh medium containing 3-NBA or 3-ABA was added without a further washing step. To identify the site of ROS production, additional experiments were done in the presence of rotenone, TTFA and AA. Rotenone inhibits electron flux from complex I to ubiquinone, whereas TTFA blocks electron transport from complex II to ubiquinone and AA inhibits electron flow at complex III.

The effect of 3-NBA on ROS-production and intracellular Ca2+ was additionally investigated in primary rat alveolar epithelial type II cells (AECs). The isolation method and the characterization of the cultured cells have been reported previously (Hansen et al., 2006).

Measurements of caspase activity

The rhodamine 110 derivative $(Asp)_2$-rhodamine 110 (Molecular Probes) allows the measurement of caspase activity in intact cell cultures. It serves as a substrate for several apoptosis-related proteases, including caspase-3 and -7. After treatment with 3-NBA for 2 hours the culture medium was removed and fresh medium containing 10 µmol/L $(Asp)_2$-rhodamine 110 was added at for another 2 hours without a further washing step. The cells were then harvested by scraping, washed with PBS and analyzed by flow cytometry.

Measurements of intracellular calcium

A549 cells and primary rat AECs were stained with Fluo-3/AM at a final concentration of 1 µmol/L for 30 min after treatment with 3-NBA without changing the culture medium. The cell permeant acetoxymethyl ester is cleaved to the cell impermeant fluorescent calcium indicator Fluo-3 by intracellular esterases. Determination of Fluo-3 fluorescence was done by flow cytometry.

Mitochondrial membrane potential measurements

Alterations in the mitochondrial membrane potential were investigated with rhodamine 123, a mitochondrial stain. A549 cells were treated with 1 µg/ml culture medium for 60 min at 37 °C prior to incubation with 3-NBA. The culture medium was then removed and fresh medium containing 3-NBA was added without a further washing step.

Determination of ROS

DCFH-DA has been widely used as a probe for H_2O_2 but oxidation by other ROS, e.g. peroxynitrite or peroxyl radical has also been reported. Superoxide anion and hydroxyl radical do not directly oxidize DCFH (LeBel et al., 1992). However, it has been shown that DCF can be directily oxidized by horseradish peroxidase and, in the presence of a reducing agent, generate superoxide and subsequently H_2O_2 (Rota et al., 1999). DCFH can thus not be used to identify the ROS species formed. Considering these limitations, DCFH can be used as an indicator of overall oxidative stress when negative controls are employed to prevent false positive results. The diacetate ester form diffuses through the cell membrane and is then de-acetylated by intracellular esterases to form nonfluorescent 2',7'-dichlorofluorescine DCFH. In the presence of ROS, DCFH forms the highly fluorescent two-electron oxidation product 2',7'-dichlorofluoresceine (DCF). DCFH-DA was added at 20 µmol/L to A549 cell cultures or

AECs 30 min prior to treatment with 3-NBA or 3-ABA and cells were then incubated at 37 °C. Cells were subsequently harvested for flow cytometric measurements.

Flow cytometry

Flow cytometry measurements were done with a FACScan cytometer (Becton Dickinson) equipped with a 488 nm argon laser. The CELLQuest™ software was used for data acquisition. For each sample, 10,000 events were analyzed and fluorescence emission of DCF, rhodamine 110, rhodamine 123 and Fluo-3 was examined at 530 nm, i.e. in the FL-1 channel. The mean fluorescence channel of all events was determined using CELLQuest™.

Cell cycle analysis

DNA content was analyzed by flow cytometry using a commercially available kit (CycleTEST™, Becton Dickinson) according to the manufacturer's instructions. The percentage of cells in the different phases of the cell cycle was calculated with the ModFit^{LT} software (Becton Dickinson).

Cell proliferation

A549 cells were seeded on 6-well culture plates and 6 µmol/L 3-NBA were added to the culture medium at various time points after passage. The cell number was determined in all wells at 8, 24, 48 and 72 hours after passage by manual counting using a Zeiss Axiovision 25 microscope equipped with a CCD camera and an image analysis system (AxioVision).

Comet assay

The alkaline comet assay was performed with subconfluent cultures of A549 cells, i.e. 24 h after passage. The cells were treated with 3-NBA or 3-ABA at 6 µmol/L and 100 nmol/L for 1 hour and subsequently harvested by trypsinization. Ethylmethane sulfonate (1 µl/mL) was used as positive control. Approximately 2 x 10^5 cells were mixed with 75 µL of low melting point

agarose (LMA, 0.75 % w/v in PBS) and loaded onto a microscopic slide precoated with normal melting point agarose (0.5 % w/v in PBS). A second layer of 80-100 µL LMA was added after gelation of the first layer. After lysis at 4 °C (2.5 M NaCl, 100 mM Na_2EDTA, 10 mM Tris, supplemented with 1 % Triton X-100 and 10 % DMSO), unwinding of the DNA was performed for 20 min at room temperature in a buffer containing 300 mM NaOH and 1 mM Na_2EDTA. Alkaline electrophoresis was performed in the same buffer for 20 min with 25 V and 300 mA. The slides were then washed three times with neutralization buffer (0.4 M Tris, pH 7.4). To visualize and determine the DNA damage, the slides were stained with ethidium bromide (20 mg/mL, 10 min). One hundred nuclei were scored per slide using a Zeiss fluorescence microscope coupled to a CCD camera and an image analysis system (Comet assay III, Perceptive Instruments, UK).

EROD activity

Determination of 7-ethoxyresorufin-*O*-deethylation (EROD) activity was done fluorimetrically. After pretreatment with 3-NBA, the culture medium was removed and fresh medium containing the substrate at 10 µmol/L was added for 1 hour. The incubation was stopped by removal and immediate freezing of the cell culture supernatant at –20 °C. Product formation (resorufin) was monitored using a VersaFluor fluorimeter (Biorad) by applying an excitation wavelength of 515 nm and an emission wavelength of 610 nm. Fluorescence was converted to pmol metabolite formation with a calibration curve for resorufin (range: 5-100 nmol/L).

Statistics

Statistical calculations were done with the SAS program package version 6.12 (SAS Institute, Cary, NC, USA) running on an AlphaServer computer model 2000 4/233 (Digital Equipment Corporation) with the operating system OpenVMS AXP, Version 7.1. If not otherwise indicated in the figure legends, data were analyzed using analysis of variance (ANOVA) with DUNNETT's t-test.

Results

Metabolism of 3-NBA by A549 cells

3-NBA was effectively metabolized by A549 cells during a 24-h incubation period (Table 1). 3-ABA was the main metabolite accounting for 95 ± 3 % of all metabolites detected in the culture medium, followed by small amounts of 3-acetylaminobenzanthrone. The enzyme inhibitors allopurinol and dicumarol did alter the metabolism of 3-NBA during a 24 hours incubation period (Table 1). For practical reasons, 3-NBA and its metabolites were analyzed in the cell culture medium only and not in the intracellular fraction, as a comprehensive analysis of 3-NBA's metabolism by A549 cells was beyond the scope of this study. However, it was important to show that A549 cells are metabolically competent towards 3-NBA because metabolic activation is likely to be an important step in 3-NBA's mechanism of action. Between 65 and 70 % of the initial dose were recovered in the cell culture medium (Table 1). Even though it is likely that the remaining 30 to 35 % represent in large part the intracellular fraction, we cannot rule out the existence of other metabolites than those analyzed by our HPLC method.

Effect of 3-NBA on apoptosis signaling

To investigate the effect of 3-NBA on caspase activity in A549 cells we used a cell-permeable caspase substrate, $(Asp)_2$-rhodamine 110. Upon caspase cleavage, the nonfluorescent substrate is converted to rhodamine 110 leading to an increase in fluorescence. The mean rhodamine 110 fluorescence was 2-fold significantly increased upon treatment with 6 µmol/L 3-NBA ($p < 0.01$, Figure 1). To test the hypothesis that activation of caspases might be directly mediated by 3-NBA-induced ROS generation, we investigated the effect of 1 mM H_2O_2. This unphysiologically high concentration was used as a positive control for oxidative stress.

Relative DCF fluorescence was increased by 190 % in H_2O_2 treated cells and by 270 % after treatment with 3-NBA with respect to untreated controls. Unexpectedly, the activity of caspases was reduced to 81 ± 4 % of untreated controls (Figure 2), suggesting that other mechanisms contribute to the activation of the apoptotic cascade in response to 3-NBA.

It has been proposed that initiation of apoptosis in various apoptotic systems requires a rise in the intracellular calcium concentration as a stimulus for downstream events. We thus considered altered [Ca^{2+}] homeostasis as a potential target of the toxic action of 3-NBA. [Ca^{2+}] levels were analyzed with Fluo-3, which is a Ca^{2+}-sensitive fluorescent dye. Fluo-3 fluorescence was increased by 60 % when compared to controls ($p < 0.05$) upon treatment with 3-NBA for 120 min (Figure 1). Mitochondrial membrane depolarization is thought to be an early event in apoptosis. Changes in the mitochondrial membrane potential were measured by flow cytometry using the potential-sensitive mitochondrial stain rhodamine 123. Rhodamine 123 is known to be accumulated in the mitochondria of living cells depending on the mitochondrial membrane potential. Mitochondrial membrane depolarization thus results in a decrease in rhodamine 123 fluorescence. 3-NBA caused a mild decrease in rhodamine 123 fluorescence (Figure 3), which was statistically significant at 120 min.

Effects of 3-NBA on cell cycle control

For cell cycle analysis, A549 cells were treated with 6 µmol/L 3-NBA for different time intervals and the cell cycle distribution was subsequently analyzed by flow cytometry. Effects of 3-NBA on the cell cycle were compared to those of the well known carcinogen benzo[*a*]pyrene (BP). Treatment of A549 cells with 3-NBA or BP (6 µmol/L) was started 48 hours after passage. After 4 hours of treatment, 62.4 ± 4.4 % of control cells were in G0/G1 phase of the cell cycle, 28.5 ± 4.3 % were in the S-phase and 9.2 ± 0.8 % were in G2/M (Table 2).The percentage of cells in G2/M was significantly reduced upon treatment with 3-NBA

alone or in combination with dicumarol, when compared with controls. Addition of SKF525A did completely reverse the effect of 3-NBA. After 24 hours of treatment, i.e. 72 hours after passage, the cell cycle distribution in control cultures was shifted towards resting cells (75.4 ± 4.2 % G0/G1,18.1 ± 2.2 % S and 5.2 ± 1.0 % G2/M). Treatment with 3-NBA then resulted in an increase in the percentage of S-phase cells to 31.1 ± 1.9 % and none of the inhibitors did prevent this increase. The same effect was observed after treatment with BP.

Effects of 3-NBA on cell proliferation

In order to aid interpretation of the cell cycle analysis experiments, we studied the effect of 3-NBA on cell proliferation of A549 cells. 3-NBA was added to the cell cultures at different time points after passage and the cells were counted at 8, 24, 48 and 72 hours. As shown in Figure 4, cell proliferation was significantly inhibited if 3-NBA (6 µmol/L) was added 4 - 24 h after passage. In contrast, addition of 3-NBA at 48 hours after passage did not change the cell growth curve, thus pointing to a proliferation-dependent toxicity to dividing cells.

Induction of DNA damage

The results of the alkaline comet assay are shown in Figure 5. A549 cells were used the day after passage, i.e. before the cell cultures reached confluency. 3-NBA (6 µmol/L) led to an increase in the mean tail moment (by 130 %), but this effect was beyond the level of statistical significance. In contrast, 3-ABA caused a significant increase in mean tail moment ($p < 0.05$) at both concentrations tested, the levels being 340 % (6 µmol/L) and 90 % over controls (0.1 µmol/L).

3-NBA and its main metabolite 3-ABA induce production of ROS in A549 cells

It is well known that apoptosis can be stimulated by ROS via the intrinsic pathway leading to permeabilization of the outer mitochondrial membrane and subsequent activation of caspase-9

and downstream caspase-3. Furthermore, ROS can cause DNA damage and this might inhibit cell cycle progression by initiating checkpoint responses. We thus investigated ROS production by human lung epithelial A549 cells by flow cytometry using the fluorogenic dye DCFH. Dose respose studies revealed, that significant increases in DCF fluorescence were measureable at 100 nmol/L 3-NBA (Figure 6). At 6 µmol/L 3-NBA caused a significant increase in DCF fluorescence (Figure 6 and 7A) as early as 30 min after addition. 3-ABA was shown to increase ROS production by more than 400 % (Figure 7B). After treatment of A549 cells with 100 nmol/L 3-ABA, a moderate increase (20 % over controls) in DCF fluorescence was observed (Figures 7D).

Effect of enzyme inhibitors on 3-NBA- and 3-ABA-mediated ROS production

As outlined above, the cytosolic reductases xanthine oxidase and NQO1 as well as cytochrome P450s may contribute to the metabolism of 3-NBA. We therefore used specific inhibitors of these enzymes to elucidate whether ROS production is linked to metabolic conversion of 3-NBA. A549 cells were used the day after passage and preincubated for 3 hours with various enzyme inhibitors before 3-NBA or 3-ABA was added for 30 min at 6 or 0.1 µmol/L. At the high concentration, allopurinol (10 µM) caused a slight reduction in 3-NBA-induced ROS production by 29 %, but this effect was not statistically significant. Addition of 10 µmol/L dicumarol reduced ROS production significantly by 57 % ($p < 0.05$), indicating that metabolism of 3-NBA by NQO1 contributes to 3-NBA-induced ROS production. Resveratrol has been reported to be a specific inhibitor of CYP1A1 (Chun et al., 1999) showing over 50-fold selectivity over CYP1A2, while SKF525A is a nonspecific inhibitor, covering a wide range of cytochrome p450s (Emoto et al., 2005). SKF525A and resveratrol reduced 3-NBA-mediated ROS production by 60 and 90 % ($p < 0.05$), respectively, suggesting that CYP1A1 may be involved in the metabolic activation of 3-NBA and concomitant ROS production

(Figure 7A). In contrast, none of the inhibitors used did affect ROS production induced by the 3-NBA metabolite 3-ABA (6 µmol/L, Figure 7B).

At a concentration of 0.1 µmol/L, 3-NBA did not cause a statistically significant increase in intracellular ROS. (Figure 7C). Upon exposure to 0.1 µmol/L 3-ABA together with dicumarol or SKF525A, intracellular ROS increased mildly. (Figure 7D).

Induction of EROD activity by 3-NBA

Resveratrol is known to inhibit CYP1A1 enzyme activity. The observed inhibition of 3-NBA-induced ROS production by resveratrol thus alludes to a potential role of CYP1A1 in the 3-NBA-induced oxidative stress response. CYP1A1 was shown to be constitutively expressed in A549 cells (Hukkanen et al., 2000) at the mRNA level and was 56-fold induced by TCDD. We therefore investigated whether 3-NBA is able to induce CYP1A1 activity and might thereby enhance its own metabolism and the resulting oxidative damage. In order to answer this question, we used the CYP1A1 marker substrate 7-ethoxyresorufin to assess 3-NBA's potential to induce CYP1A1 enzyme activity. As shown in Figure 8, EROD activity was 90 % and 30 % greater in A549 cells pretreated with 6 µmol/L and 0.1 µmol/L 3-NBA for 24 hours, respectively, than in control cultures. The well known CYP1A1 inducer Aroclor 1254 was used as a positive control at 10 µmol/L, but its effect was less pronounced compared to 6 µmol/L 3-NBA.

Effects of the iron chelator DFO on 3-NBA- and 3-ABA-induced ROS production

The potent iron chelator DFO is taken up by endocytosis (Lloyd et al., 1991; Cable and Lloyd, 1999) and is then distributed to the lysosomal compartment (Kurz et al., 2004). Lysosomal membrane destabilization and rupture can occur as a consequence of iron-catalyzed intralysosomal oxidative reactions (Tenopoulou et al., 2005). Pretreatment of A549 cells with 10 µmol/L DFO prior to treatment with 6 µmol/L 3-NBA or 3-ABA significantly reduced 3-

NBA-induced ROS production by 78 % ($p < 0.05$), whereas 3-ABA-induced ROS production was not affected (Figure 7A and 7B). As DFO is not able to pass cellular membranes by passive diffusion, it should have little effect on cytosolic or mitochondrial ROS production. Thus, the observed reduction of 3-NBA-induced ROS production by DFO suggests that intralysosomal Fenton type reactions contribute substantially to the oxidative stress response triggered by 3-NBA.

Effects of inhibitors of the mitochondrial electron transport chain on 3-NBA-induced ROS production

In order to investigate whether the mitochondrial respiratory chain contributes to 3-NBA-induced ROS generation, we used the respiratory chain inhibitors rotenone, TTFA and AA. When rotenone alone (10 µmol/L) or rotenone and TTFA (10 µmol/L each) were added together with 3-NBA, DCF fluorescence was significantly reduced by about 20 % ($p < 0.05$, Figure 9). This suggests that the site of interaction is distal to complex I. AA had no effect on 3-NBA-induced ROS production, indicating that complex III is not involved in ROS production upon 3-NBA exposure.

Results with primary rat AECs

The effects of 3-NBA on ROS-production and intracellular calcium were additionally investigated in primary rat AECs and the results are shown in Figure 10. Treatment with 3-NBA at 6 µmol/L for 30 min caused an increase in DCF fluorescence by 150 % ($p < 0.05$) while calcium-dependent Fluo-3 fluorescence was increased by 100 %. These results confirm that the responses of primary lung epithelial cells regarding ROS generations and calcium homeostasis are similar to those of immortalized carcinoma cells.

Discussion

In the present study, we have shown that metabolism of 3-NBA and its main metabolite 3-ABA by human lung epithelial A549 cells is associated with significantly increased ROS production. Enzyme inhibition studies provided evidence that NQO1 is one of the enzymes involved in the metabolic activation of 3-NBA. At low concentrations (100 nmol/L), ROS production by 3-NBA was slightly increased by addition of dicumarol. This implies that the antioxidant activity of NQO1 is predominant when low substrate concentrations are used. In contrast, at the high and possibly unphysiological concentration of 6 µmol/L, NQO1 might contribute to ROS production rather than prevent it. 3-ABA-induced ROS production was not affected by dicumarol, suggesting that NQO1 is not involved in the metabolic activation of 3-ABA. This is in agreement with earlier findings (Arlt et al., 2004 and 2006) that 3-ABA is primarily activated by CYP1A1 and CYP1A2. It is unclear, why allopurinol and dicumarol had no effect on the conversion of 3-NBA to 3-ABA (as shown in table 1 after 24 hours), but decreased ROS-production. However, this question cannot be answered without speculation. It is possible that other enzymes than those known to date contribute to the metabolism of 3-NBA. Furthermore, ROS-production is a rapid phenomenon and was measured 30 min after treatment with 3-NBA or 3-ABA. Unfortunately, metabolite formation could not be quantified reliably in the cell culture medium after that short incubation time, because the metabolite concentrations were below the LOQ of the analytical method.

The observed reduction of ROS production by SKF525A and resveratrol points to an involvement of cytochrome P450s and especially CYP1A1 and CYP1A2 in the oxidative stress response triggered by 3-NBA and 3-ABA. Resveratrol, which is found in grapes and red wine, has been shown to inhibit CYP1A1 and CYP1A2 at the level of enzyme activity (Ciolino and Yeh, 1999; Chang et al., 2001). However, it is well documented, that resveratrol has also

antioxidant properties and the observed decrease of ROS formation may thus partly be caused by direct ROS scavenging. To estimate the impact of resveratrol's direct antioxidant activity in our experimental system, DCF fluorescence was analysed in A549 cell cultures after treatment with H_2O_2 with and without resveratrol pretreatment (data not shown). It was shown in these preliminary experiments, that H_2O_2 induced DCF fluorescence was not affected by resveratrol. We thus conclude that the observed effect of resveratrol on 3-NBA-induced ROS-formation may, at least in part, be due to CYP1A1 inhibition. It is noteworthy that we observed induction of CYP1A1 enzyme activity by 3-NBA using the EROD assay, even though 3-NBA-induced ROS should be expected to repress CYP1A1 activity (Barouki et al., 2001). Expression of the NQO1 gene is controlled by the antioxidant response element (ARE), a distinct regulatory element in the 5'-flanking region of the NQO1 gene, which is activated by electrophiles and ROS (Nguyen et al., 2003). Exposure to 3-NBA or 3-ABA could thus lead to enhanced NQO1 expression due to the oxidative stress response, which in turn could further enhance 3-NBA activation and its genotoxic potential. Furthermore, other contaminants on the surface of diesel exhaust particles (DEP), such as PAH and PAH-derived quinones, are also able to induce ROS production in cells of the respiratory tract, thereby enhancing the toxicity of 3-NBA. Induction of CYP1A1 and NQO1 gene expression by DEP in human bronchial epithelial 16HBE cells has been reported (Baulig et al., 2003), and it was shown that the organic part of DEP is responsible for these effects. Furthermore, in a recent study Stiborova et al. (2006) demonstrated that 3-NBA and 3-ABA are both potent inducers of hepatic CYP1A1 and CYP1A2 as well as NQO1 in male Wistar rats. The authors come to the conclusion that this mechanism could be important as both compounts might enhance their own metabolism to reactive DNA-binding species and thus their genotoxic potential. Concerning the results of the present study, induction of the main enzymes responsible for 3-NBA's and 3-ABA's

metabolism could also enhance the formation of ROS during extendet environmental exposure to 3-NBA.

Within the cell, redox active iron (low molecular weight iron, not ferritin bound) is essentially located within the acidic lysosomal compartment and it is carefully kept there, because iron-catalyzed oxidation reactions are an important mediator of oxidant-induced cell death. The observed reduction of ROS production by DFO suggests that intralysosomal iron plays an important role in the 3-NBA-mediated oxidative stress response at least when 3-NBA is present at high substrate concentrations. However, the importance of intralysosomal iron in 3-NBA's toxicity might influence the toxic potential of 3-NBA depending on the exposure to particulate air pollution. Recently, it has been proposed that disruption of iron homeostasis is a common mechanism of the biologic effects of many ambient air pollution particles (Ghio et al., 2005). Exposure to particulate air pollution in urban areas could thus enhance the cancer risk associated with diesel exhaust and in particular 3-NBA. Furthermore, particles from different urban subenvironments can differ in their composition and some do contain considerable amounts of iron (Karlsson et al., 2005). Moreover, the susceptibility towards iron-mediated oxidative stress of different cell types of the respiratory tract is highly variable. For instance, it has been reported that A549 cells exhibit a higher resistance to oxidative stress than bronchial epithelial cells, due to a higher content of the iron-chelating protein ferritin (Persson et al., 2001). The oxidative burst upon 3-NBA exposure might thus be higher in other respiratory cell types, such as nasal or bronchial epithelial cells, caused by a reduced capability of these cells to chelate intralysosomal iron.

ROS are known to play a dual role in apoptosis. While mild oxidative stress is a reproducible inducer of apoptosis (Hoidal et al., 2001; Lau et al., 2004), excessive oxidative stress can

actually prevent apoptosis (Hampton and Orrenius, 1997). This is plausible, because the key enzymes in the apoptosis cascade, caspases, are cysteine-dependent enzymes and thus redox sensitive. 3-NBA caused a significant increase in caspase activity and in intracellular [Ca^{2+}]. Furthermore, 3-NBA was shown to cause depolarization of the mitochondrial membrane. We thus suggest that alveolar epithelial cell apoptosis contributes to 3-NBA-induced lung injury. The mitochondrial electron transport chain is a major source of ROS generated "accidentally" during respiration. As mitochondrial ROS production is especially important during apoptosis, we investigated the impact of mitochondrial ROS production on 3-NBA's mechanism of action. We could demonstrate that mitochondrial ROS production contributes to the 3-NBA-dependent oxidative stress response, but only to a small extent of about 20 %.

When growing cells are damaged, they have the possibility to pause temporarily in the G1, S or G2 phases of the cell cycle to repair the damage and then re-enter the cell cycle. The so-called G1 checkpoint depends on activation of the p53 gene product and can be induced by oxidative stress (Kastan et al., 1991). Cell cycle analysis experiments revealed that 3-NBA caused a slight decrease in the percentage of cells in G2/M after 4 hours of treatment. After 24 hours of treatment, the percentage of cells in the S-phase was significantly increased in 3-NBA-treated cell cultures. Considering the results of the proliferation experiment (Figure 4), it is obvious that this effect is caused by a reduction of the total cell number immediately after addition of 3-NBA - the remaining cells proliferated more actively after 24 hours, whereas control cultures already reached confluence at that time point. It should be kept in mind, however, that A549 cells are a transformed cell line with altered cell cycle regulation capacities. It is likely that the effects of 3-NBA on normal alveolar epithelial cells would be less intense. The high toxicity towards proliferating cells is consistent with 3-NBA's ability to damage DNA, either directly by formation of 3-NBA-derived DNA adducts or via ROS. The ability of 3-NBA to produce

DNA damage in A549 cells was confirmed by the results of the alkaline comet assay. This is consistent with previous studies, where 3-NBA was shown to cause DNA damage in A549 cells by alkaline comet assay with FPG-treatment (Nagy et al., 2005). Furthermore, the genotoxicity of 3-NBA was previously documented in several short term assays (Arlt et al., 2005). Interestingly, we observed that the main metabolite 3-ABA was more effective in producing DNA damage than the parent compound. Considering the ability of 3-ABA to induce ROS generation in A549 cells, the observed DNA damage is most probably caused by ROS. The observation that 3-ABA contributes directly to the genotoxic potential of 3-NBA is in line with previous studies providing evidence for DNA adduct formation by 3-ABA.

The fact that 3-ABA can act as a genotoxic carcinogen per se and is also able to induce the production of ROS in alveolar epithelial cells emphasized the importance of 3-NBA as risk factor for human lung cancer. The parent compound 3-NBA is relatively unstable in the environment and has been shown to be subject to photolysis (Feilberg et al., 2002) and rearrangement to its isomer 2-nitrobenzanthrone (Phousongphouang and Arey, 2003; Tang et al., 2004). Direct human exposure to high concentrations of 3-NBA by inhalation is therefore not likely. In contrast, the main metabolite of 3-NBA, 3-ABA, has been detected in urine samples of salt mining workers occupationally exposed to 3-NBA in considerable concentrations (1 - 143 ng/24h urine, Seidel et al., 2002). This suggests that 3-ABA is readily bioavailable in the systemic circulation and may thus reach its target cells in higher amounts than 3-NBA. It is not known to date, which concentrations of 3-NBA or its metabolites are reached in target cells under common occupational or environmental exposure conditions. Hence, the relevance of the concentrations studied to the human in vivo situation cannot be completely evaluated at present. However, at least the dimension of the concentrations used in this study is indeed comparable to recent *in vivo* studies with rats. For example, Nagy et. al.

(2006) administered a single oral dose of 1 mg to Fischer F344 rats of approximately 110 g. Assuming that only 1 % of this dose might become bioavailable in the systemic circulation at a certain time point and assuming a total blood volume of 60 ml/kg, this would lead to a blood concentration of 1.5 µg/mL blood corresponding to 5.4 µmol/L. Nevertheless, concentrations in the micromolar range are most likely far above those reached in humans in common exposure scenarios. These studies aim at investigating the molecular mechanism of 3-NBAs mode of action. Furthermore, for DNA-binding agents, cumulative dose exposure is often more closely correlated with biological effects then are short term concentrations of the primary compund.

Taken together, the results of the present study suggest that 3-NBA and its main metabolite 3-ABA are able to produce oxidative stress in human epithelial lung cells. This increased oxidizing environment in the lung could greatly contribute to the initiation and promotion of cells to neoplastic growth. The relevance of our *in vitro* results to the in vivo situation has to be established by *in vivo* experiments. The ability of 3-NBA to induce CYP1A1 has already been confirmed in a recent *in vivo* study with rats (Stiborova et al., 2006). Further animal studies are warranted to investigate the effects of 3-NBA and 3-ABA on cell cycle control and their potential to induce apoptosis in lung epithelial cells in vivo.

Acknowledgements

The authors thank Christina Ziemann for critical proofreading of the manuscript.

Figure 1

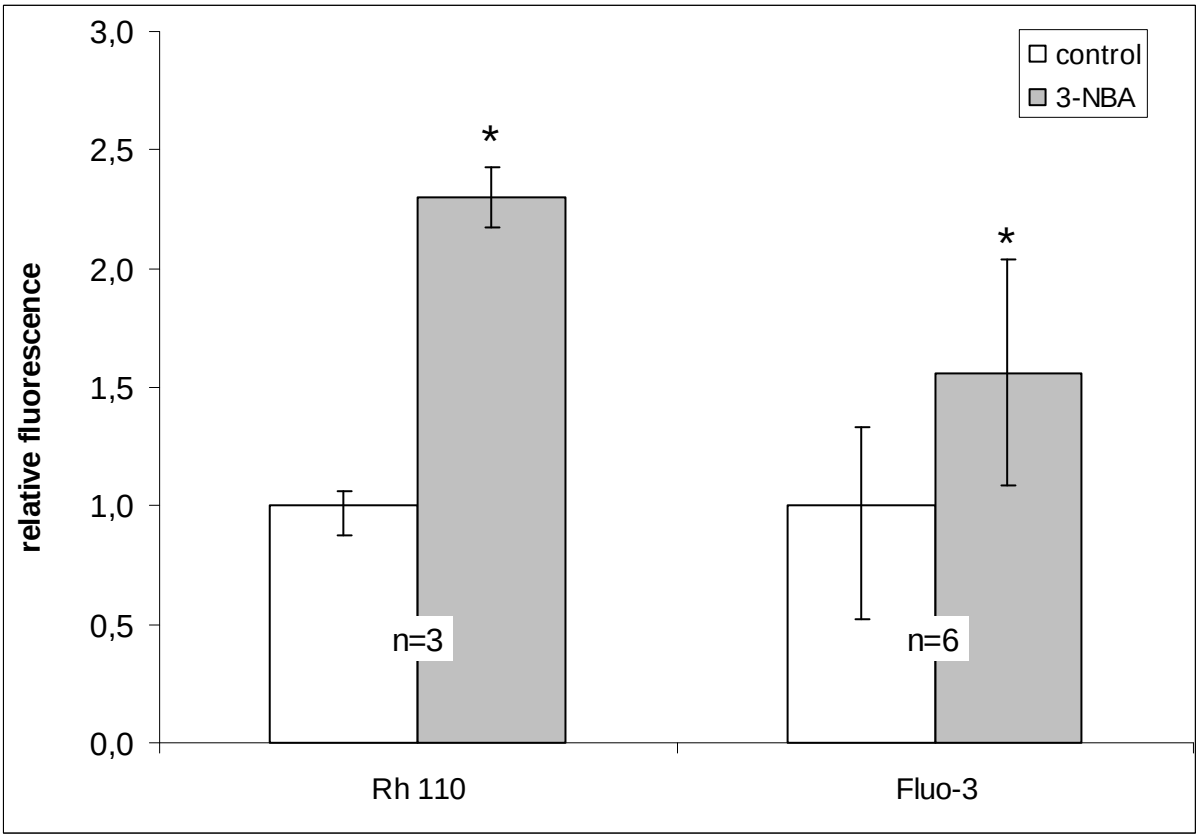
3,0
2,5
2,0
1,5
1,0
0,5
0,0
relative fluorescence
control
3-NBA
*
*
n=3
n=6
Rh 110
Fluo-3

Figure 2

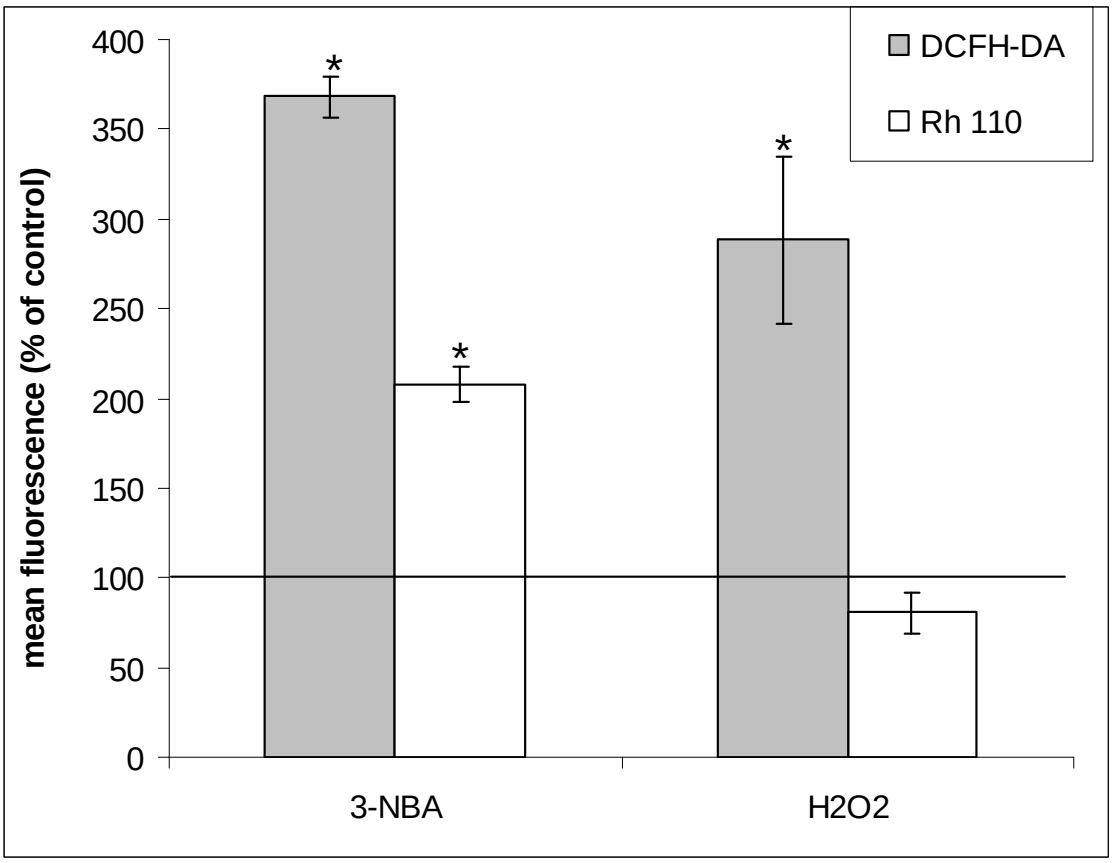
DCFH-DA
Rh 110
mean fluorescence (% of control)
400
350
300
250
200
150
100
50
0
*
*
*
3-NBA
H2O2

Figure 3

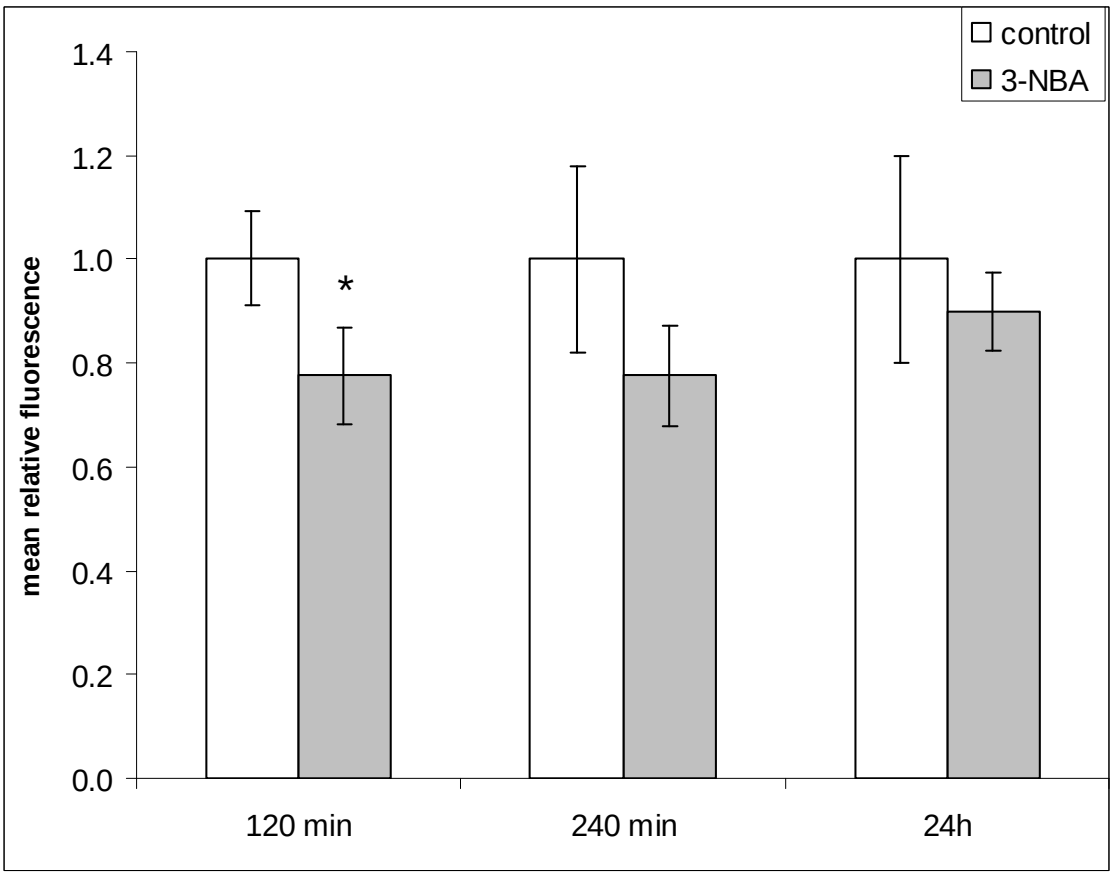
control
3-NBA
mean relative fluorescence
1.4
1.2
1.0
0.8
0.6
0.4
0.2
0.0
*
120 min
240 min
24h

Figure 4

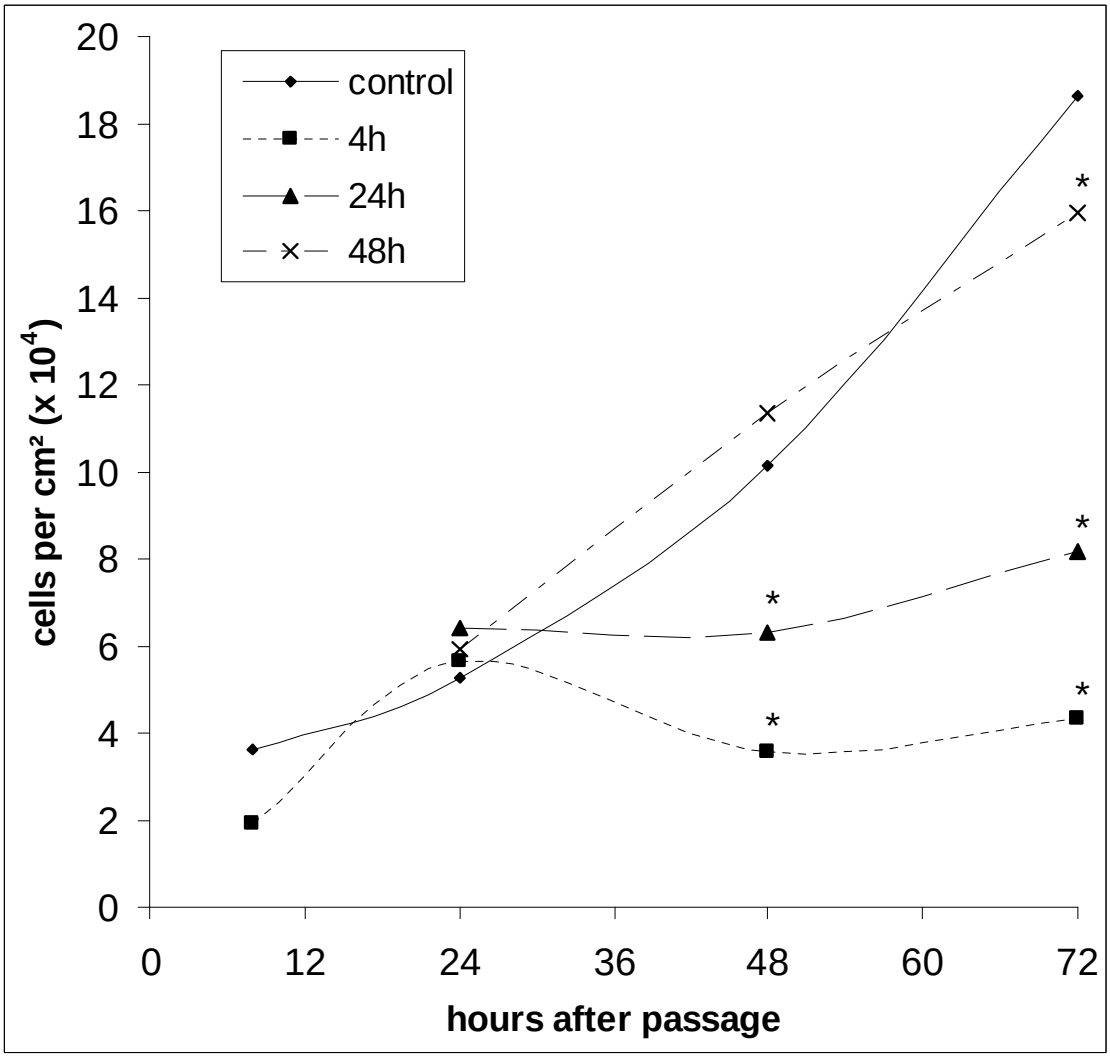
control
4h
24h
48h
cells per cm² (x 10⁴)
hours after passage
0
2
4
6
8
10
12
14
16
18
20
0
12
24
36
48
60
72
*
*
*
*
*

Figure 5

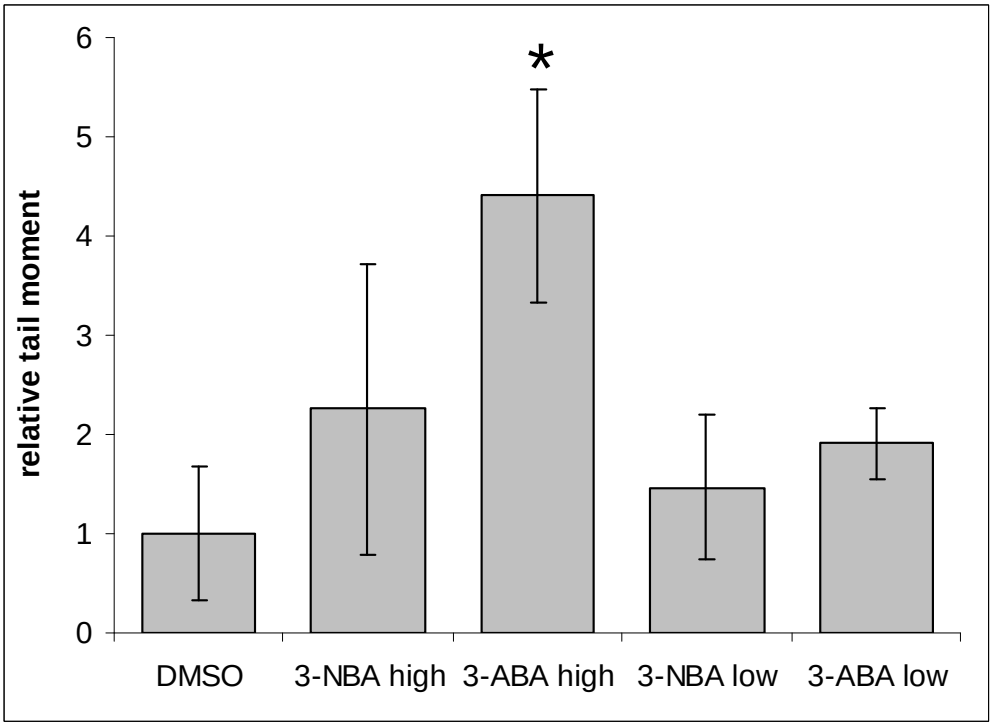
relative tail moment
6
5
4
3
2
1
0
*
DMSO
3-NBA high
3-ABA high
3-NBA low
3-ABA low

Figure 6

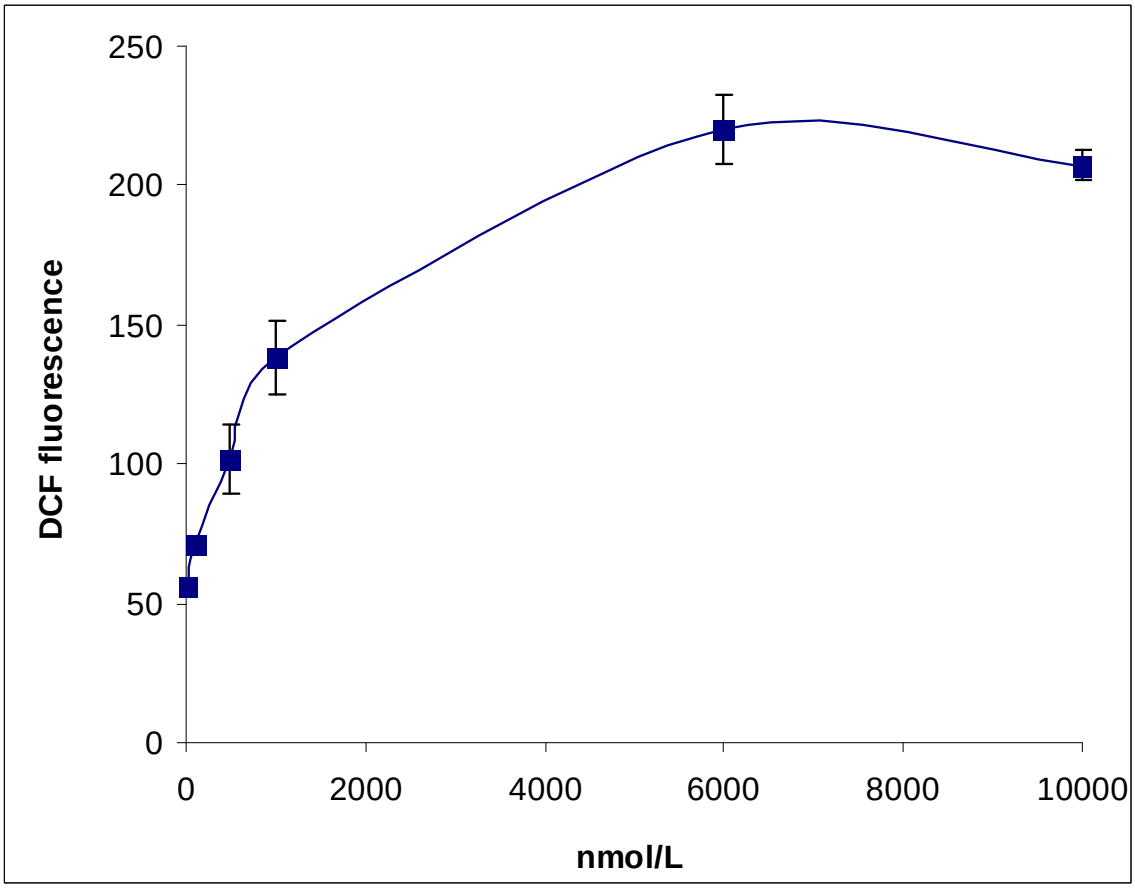
250
200
150
100
50
0
DCF fluorescence
0
2000
4000
6000
8000
10000
nmol/L

Figure 7A

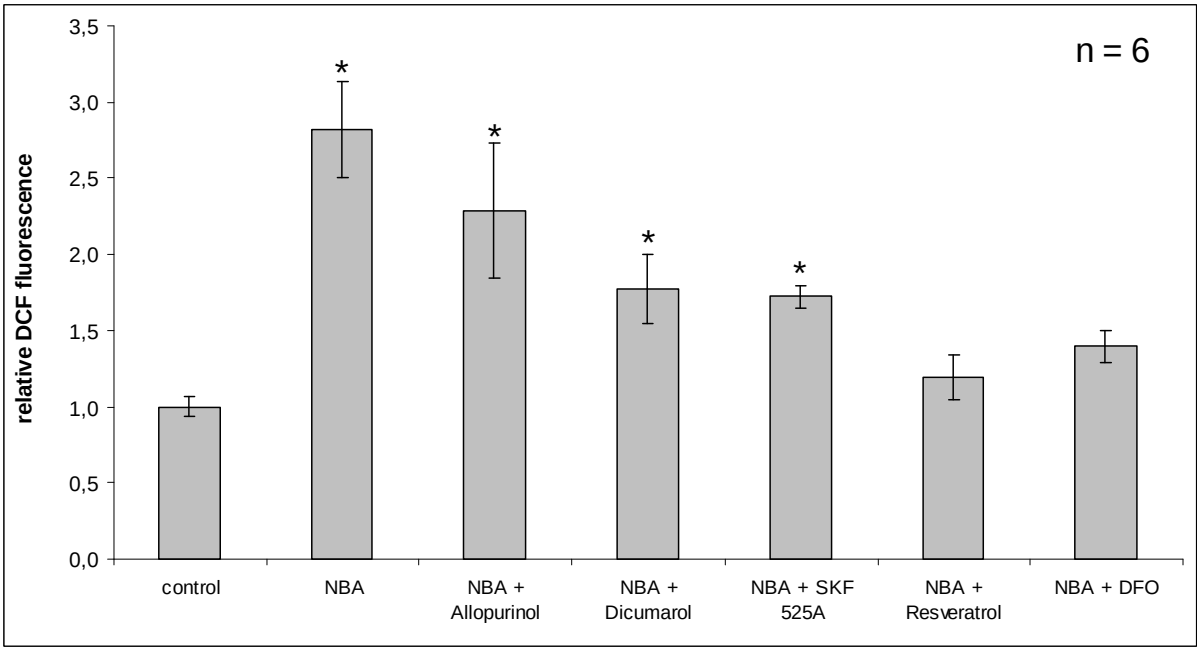

Figure 7B

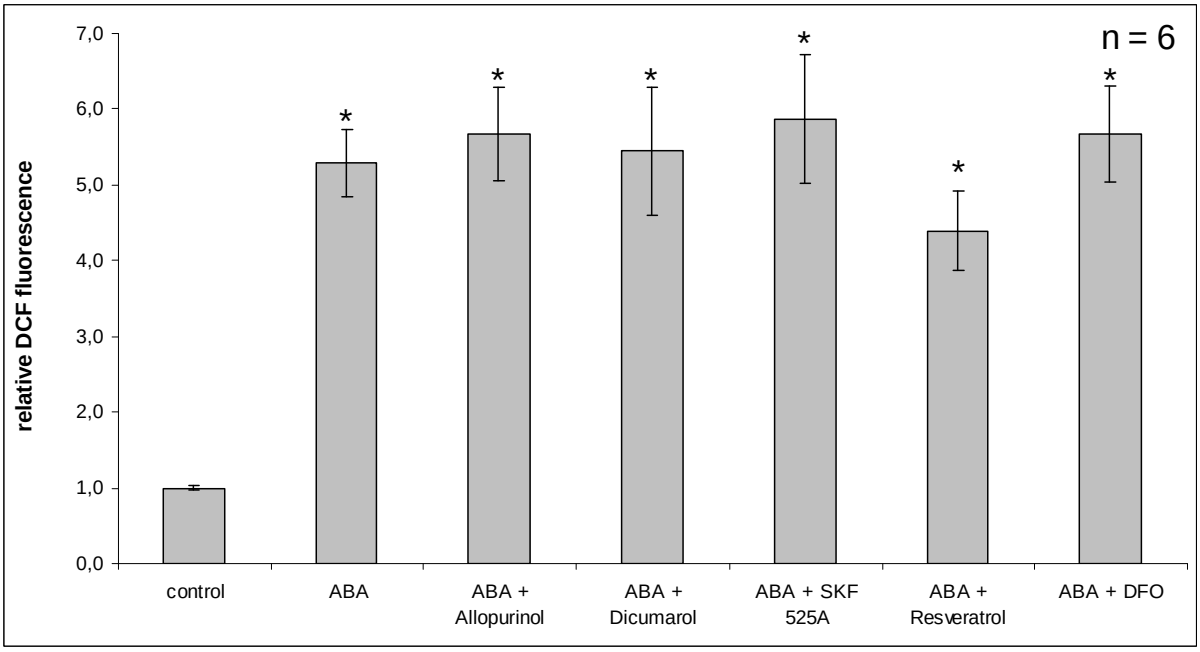

Figure 7C

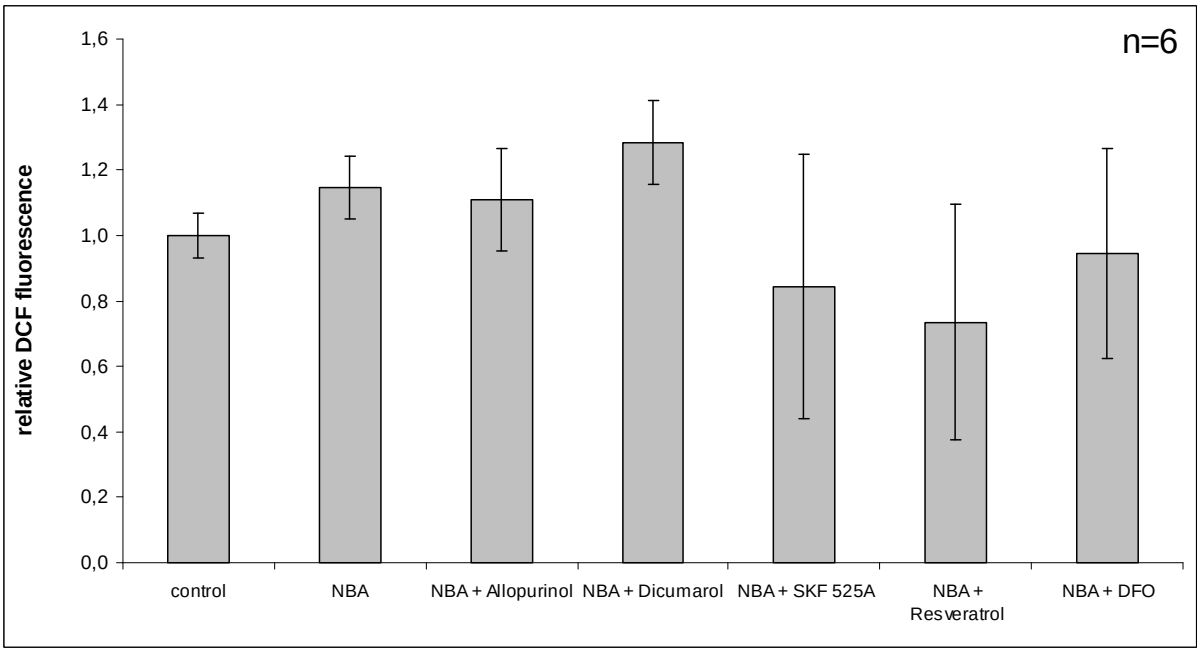

Figure 7D

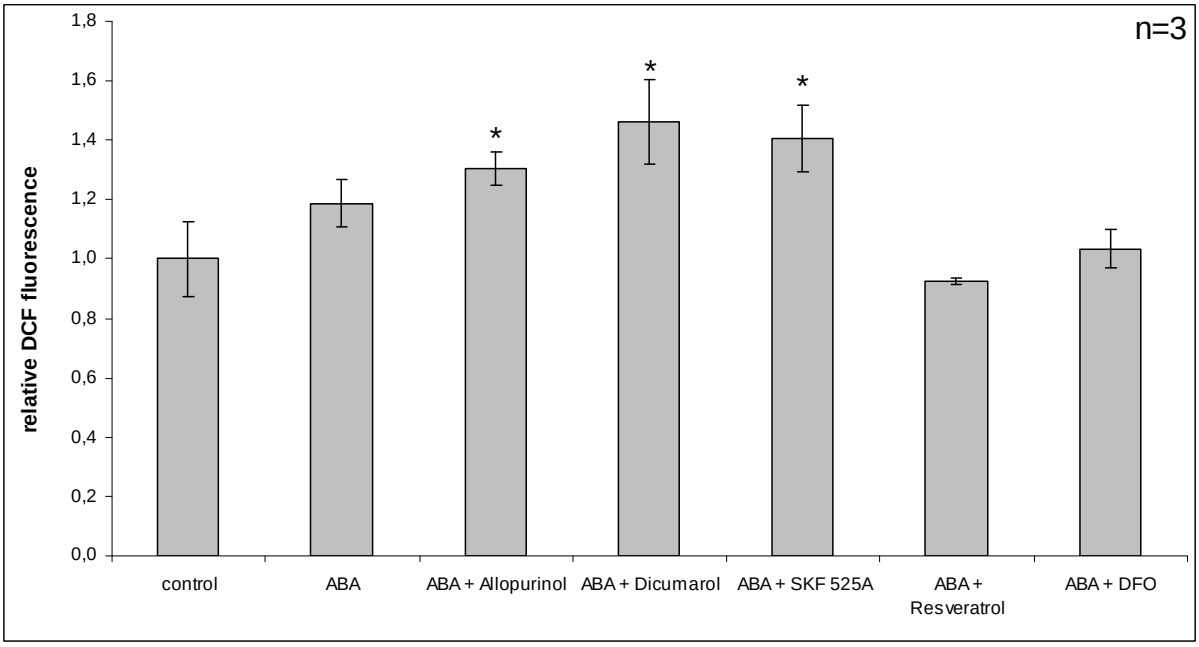

Figure 8

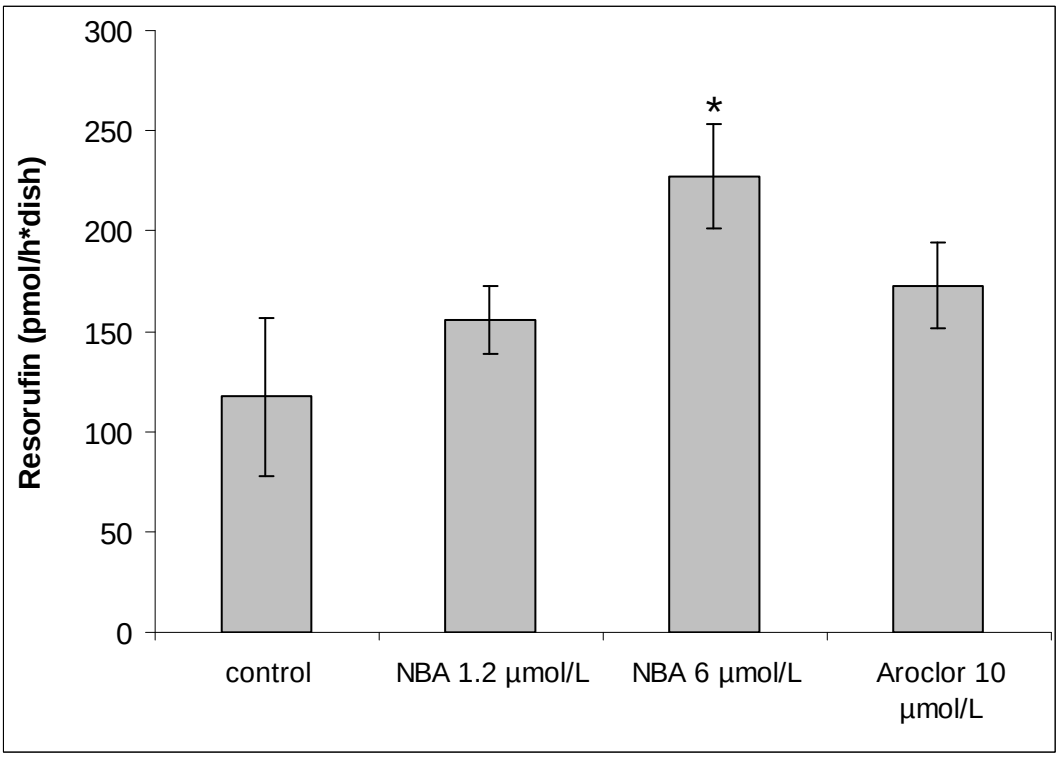
Resorufin (pmol/h*dish)
300
250
200
150
100
50
0
*
control
NBA 1.2 µmol/L
NBA 6 µmol/L
Aroclor 10 µmol/L

Figure 9

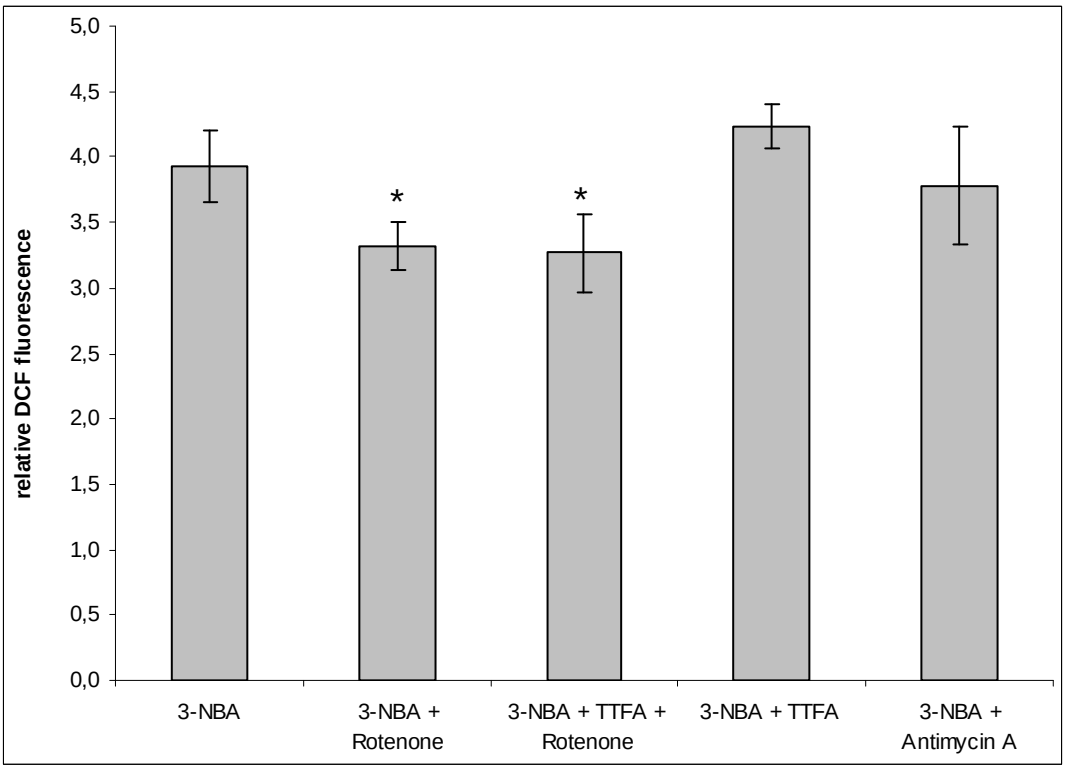
relative DCF fluorescence
5,0
4,5
4,0
3,5
3,0
2,5
2,0
1,5
1,0
0,5
0,0
*
*
3-NBA
3-NBA + Rotenone
3-NBA + TTFA + Rotenone
3-NBA + TTFA
3-NBA + Antimycin A

Figure 10

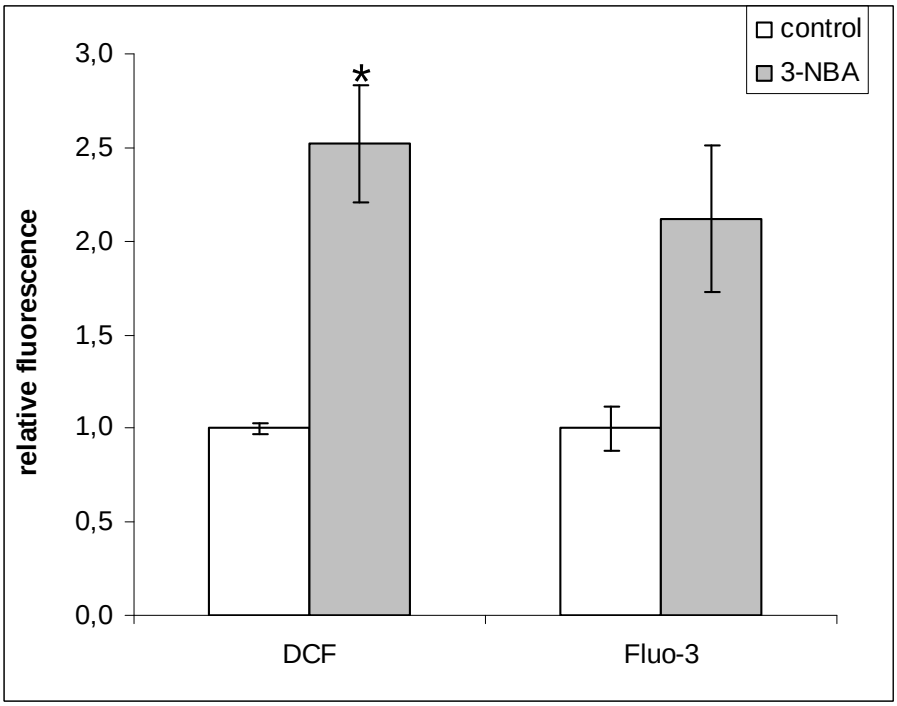
control
3-NBA
relative fluorescence
3,0
2,5
2,0
1,5
1,0
0,5
0,0
*
DCF
Fluo-3

Legends to figures

Figure 1: Effects of 3-NBA on caspase activity and intracellular calcium. A549 cells were pretreated with 3-NBA (6 µmol/L) for 2 hours. The caspase substrate $(Asp)_2$-rhodamine 110 was added at 10 µmol/L for additional 2 hours. The calcium indicator Fluo-3 was used at 1 µmol/L and incubated for 30 min. Results are given as relative fluorescence intensities normalized to untreated controls (mean and SD). * significantly different from controls, $p < 0.05$.

Figure 2: To determine whether the increase in caspase activity upon 3-NBA exposure is directly mediated by H_2O_2, A549 cells were treated with 6 µmol/L 3-NBA or alternatively with 1 mmol/L H_2O_2 for 2 hours. ROS production was subsequently analyzed with DCFH-DA, and caspase activity was assessed using $(Asp)_2$-rhodamine 110. Results are mean and SD of three measurements. Fluorescence values of untreated control cultures were set to 100 %. * significantly different from controls, $p < 0.05$.

Figure 3: Effects of 3-NBA in the mitochondrial membrane potential. A549 cells were treated with 6 µmol/L 3-NBA for different time intervals as indicated. Mitochondrial membrane depolarization was subsequently analyzed with rhodamine 123. Results represent mean fluorescence and SD of three independent measurements and are shown relative to control values. Two-way ANOVA revealed an effect of 3-NBA, no effect of time and no interaction. * significantly different from controls ($p < 0.05$ Dunnett's Test).

Figure 4: Effect of 3-NBA on cell proliferation. A549 cells were seeded on 6-well culture plates and 3-NBA (6 µmol/L) was added to the cultures at various time points after passage, as indicated in the legend. The cell number was determined by manual counting using a light microscope. Results are mean of three wells. * significantly different from controls, $p < 0.05$.

Figure 5: DNA damage in A549 cells after treatment with 3-NBA or 3-ABA at 6 µmol/L (high) or 0.1 mmol/L (low) for 1 hour as judged by alkaline comet assay. Results are mean and SD of four slides. * significantly different from controls, $p < 0.05$.

Figure 6: Dose response curve for 3-NBA induced DCF fluorescence. A549 cells were treated with 3-NBA for 30 min at different concentrations and ROS production was measured by flow cytometry with DCFH-DA (n=3). Statistical analysis with one-way ANOVA showed a strong effect of concentration ($p < 0.0001$).

Figure 7: Effect of enzyme inhibitors and DFO on 3-NBA- and 3-ABA-induced ROS production in A549 cells. Cell cultures were preincubated for 3 hours with or without the inhibitors prior to treatment with 3-NBA or 3-ABA for 30 min. ROS production was measured by flow cytometry with DCFH-DA. The dose levels of 3-NBA and 3-ABA were 6 µmol/L (7A and 7B) or 100 nmol/L (7C and 7D). Results are given as relative fluorescence intensities normalized to untreated controls. *significantly different from solvent controls.
$p < 0.05$

Figure 8: Induction of 7-ethoxyresorufin-O-deethylation (EROD) activity by 3-NBA. After a 24-hour preincubation period with 3-NBA, the substrate 7-ethoxyresorufin was added at 10 µmol/L for 1 h. Aroclor 1254 was used as a positive control for CYP1A1 induction. The production of the deethylation product resorufin was measured fluorimetrically. Results are mean and SD of 6 measurements. *significantly different from untreated controls. * $p < 0.05$.

Figure 9: Effects of inhibitors of the mitochondrial electron transport chain on 3-NBA-induced ROS production. Cell cultures were treated with 3-NBA and the various inhibitors for 2 hours and ROS production was subsequently measured by flow cytometry with DCFH-DA. Results are mean and SD of at least six measurements and are given as relative fluorescence intensities normalized to untreated controls. *significantly different from cultures treated with 3-NBA alone, * $p < 0.05$.

Figure 10: Effects of 6 µmol/L 3-NBA on ROS-production and intracellular calcium in primary rat AECs. ROS production was measured by flow cytometry with DCFH-DA (n=4). The intracellular calcium concentration was measured using the fluorescent dye Fluo-3 at 1 µmol/L (n=2). Fluo-3 was incubated for 30 min. Results are mean and SD and are given as relative fluorescence intensities normalized to untreated controls. * significantly different from controls, $p < 0.05$.

Table 1: Metabolism of 3-NBA by human lung epithelial A549 cells. 3-NBA was added to the culture medium at 6 µmol/L and incubated for 24 hours. 3-NBA and its metabolites were analyzed in the cell culture medium by HPLC. Results are shown as µmol/L and represent mean and SD of 8 independent measurements. Statistical analysis (one-way ANOVA) indicated no effect of treatment. 3-AcABA = 3-acetyl aminobenzanthrone.

	Without inhibitor	Allopurinol (10 µmol/L)	Dicumarol (10 µmol/L)
3-AcABA	0.107 ± 0.034	0.100 ± 0.035	0.084 ± 0.018
3-ABA	3.723 ± 0.464	3.753 ± 0.350	4.037 ± 0.686
3-NBA	0.075 ± 0.098	0.106 ± 0.133	0.103 ± 0.105
Recovery (% of initial dose)	65	66	70

Table 2: Effect of 3-NBA and BP on the cell cycle in human lung epithelial A549 cells. Cell cultures were treated for 4 or 24 hours with 6 µmol/L BP or 3-NBA with or without the enzyme inhibitors allopurinol, dicumarol and SKF525A (10 µmol/L). Cell cycle analysis was done by flow cytometry. Results are mean ± SD (n = 5). Statistical analysis was done by one-way ANOVA and Student-Newman Keuls test: * significantly different from controls, # significantly different from cultures treated with 3-NBA alone ($p < 0.05$)

4 hours			
	% G0/G1	% S-phase	% G2/M
control	62.4 ± 4.38	28.5 ± 4.28	9.2 ± 0.77
BP	64.4 ± 1.76	26.3 ± 2.68	9.3 ± 1.19
3-NBA	67.9 ± 1.94	24.7 ± 1.85	7.4 ± 0.72*
3-NBA + allopurinol	66.0 ± 1.0	23.0 ± 3.18	11.0 ± 2.53
3-NBA + dicumarol	67.1 ± 2.75	24.9 ± 2.41	8.0 ± 3.03*
3-NBA + SKF	63.7 ± 1.98	24.2 ± 3.83	12.1 ± 1.87#
24 hours			
	% G0/G1	% S-phase	% G2/M
control	75.4 ± 4.20	18.1 ± 2.17	5.2 ± 1.04
BP	71.4 ± 2.72	25.0 ± 2.87*	3.6 ± 2.86
3-NBA	68.8 ± 1.96	31.1 ± 1.93*	0.1 ± 0.08
3-NBA + allopurinol	70.3 ± 2.31	27.3 ± 3.57*	2.4 ± 2.94
3-NBA + dicumarol	67.7 ± 6.03	31.4 ± 5.73*	1.0 ± 1.81
3-NBA + SKF	68.1 ± 6.45	28.6 ± 3.27*	3.3 ± 3.39

References

Arlt, V.M., 2005. 3-nitrobenzanthrone, a potential human cancer hazard in diesel exhaust and urban air pollution: a review of the evidence. Mutagenesis, 20, 399-410.

Arlt, V.M., Bieler, C.A., Mier, W., Wiessler, M and Schmeiser, H.H., 2001. DNA adduct formation by the ubiquitous environmental contaminant 3-nitrobenzanthrone in rats determined by ^{32}P-postlabeling. Int. J. Cancer 93(3), 450-454.

Arlt, V.M., Glatt, H., Muckel, E., Pabel, U., Sorg, B.L. and Schmeiser, H.H., 2002. Metabolic activation of the environmental contaminant 3-nitrobenzanthrone by human acetyltransferases and sulfotransferase. Carcinogenesis 23(11), 1937-1945.

Arlt, V.M., Glatt, H., Muckel, E., Pabel, U., Sorg, B.L., Seidel, A., Frank, H., Schmeiser, H.H. and Phillips, D.H., 2003. Activation of 3-nitrobenzanthrone and its metabolites by human acetyltransferases, sulfotransferases and cytochrome P450 expressed in Chinese hamster V79 cells. Int. J. Cancer 105(5), 583-592.

Arlt, V.M., Henderson, C.J., Wolf, C.R., Schmeiser, H.H., Phillips, D.H. and Stiborova, M., 2006. Bioactivation of 3-aminobenzanthrone, a human metabolite of the environmental pollutant 3-nitrobenzanthrone: evidence for DNA adduct formation mediated by cytochrome P450 enzymes and peroxidases. Cancer Lett., 234, 220-234.

Arlt, V.M., Hewer, A., Sorg, B.L., Schmeiser, H.H., Phillips, D.H. and Stiborova,M., 2004. 3-aminobenzanthrone, a human metabolite of the environmental pollutant 3-nitrobenzanthrone, forms DNA adducts after metabolic activation by human and rat liver microsomes: evidence for activation by cytochrome P450 1A1 and P450 1A2. Chem. Res. Toxicol. 17(8), 1092-1101.

Arlt, V.M., Sorg, B.L., Osborne, M., Hewer, A., Seidel, A., Schmeiser, H.H. and Phillips, D.H., 2003. DNA adduct formation by the ubiquitous environmental pollutant 3-nitrobenzanthrone and its metabolites in rats. Biochem. Biophys. Res. Commun. 300(1), 107-114.

Arlt, V.M., Stiborova, M., Henderson, C.J., Osborne, M.R., Bieler, C.A., Frei, E., Martinek, V., Sopko, B., Wolf, C.R., Schmeiser, H.H. and Phillips,D.H., 2005. Environmental pollutant and potent mutagen 3-nitrobenzanthrone forms DNA adducts after reduction by NAD(P)H:quinone oxidoreductase and conjugation by acetyltransferases and sulfotransferases in human hepatic cytosols. Cancer Res. 65(7), 2644-2652.

Atkinson, R., and Arey, J., 1994. Atmospheric chemistry of gas-phase polycyclic aromatic hydrocarbons: formation of atmospheric mutagens. Environ. Health Perspect. 102 (Suppl 4), 117-126.

Barker, C.W., Fagan, J.B. and Pasco, D.S., 1994. Down-regulation of P450 1A1 and 1A2 mRNA expression in isolated hepatocytes by oxidative stress. J. Biol. Chem. 267, 3985-3990.

Barouki, R. and Morel, Y., 2001. Repression of cytochrome P450 1A1 gene expression by oxidative stress: mechanisms and biological implications. Biochem. Pharmacol., 61, 511-516.

Baulig, A., Garlatti, M., Bonvallot, V., Marchand, A., Barouki, R., Marano, F. and Baeza-Squiban, A., 2003. Involvement of reactive oxygen species in the metabolic pathways triggered by diesel exhaust particles in human airway epithelial cells. Am. J. Physiol. Lung Cell Mol. Physiol., 285, L671-L679.

Bieler, C. A., Wiessler, M., Erdinger, L., Suzuki, H., Enya, T. and Schmeiser, H.H., 1999. DNA adduct formation from the mutagenic air pollutant 3-nitrobenzanthrone. Mutat Res 439(2): 307-311.

Boffetta, P., Dosmeci, M., Gridley, G., Bath, H., Moradi, T. and Silverman, DS., 2001. Occupational exposure to diesel engine emissions and risk of cancer in Swedish men and women. Cancer Causes and Control, 12, 365-374.

Borlak, J., Hansen, T., Yuan, Z., Sikka, H.C., Kumar, S., Schmidbauer, S., Frank, H., Jacob, J. and Seidel, A., 2000. Metabolism and DNA-binding of 3-nitrobenzanthrone in primary rat alveolar type II cells, in human fetal bronchial, rat epithelial and mesenchymal cell lines. Polycycl. Aromat. Compds., 21, 73-86.

Cable, H. and Lloyd, J.B., 1999. Cellular uptake and release of two contrasting iron chelators. J. Pharm. Pharmacol., 51(2), 131-134.

Castell, J.V., Donato, M.T. and Gomez-Lechnon, M.J., 2005. Metabolism and bioactivation of toxicants in the lung. The in vitro cellular approach. Exp. Toxicol. Pathol., 57, 189-204.

Chang, T.K.H., Chen, L. and Lee, B.K., 2001. Differential inhibition and inactivation of human cYP1 enzymes by trans-resveratrol: evidence for mechanism-based inactivation of CYP1A2. J. Pharmacol. Exp. Ther., 299(3), 874-882.

Chien, P.S., Mak, O.T. and Huang, H.J., 2006. Induction of COX-2 gene expression by vanadate in A549 human lung carcinoma cell line through EGF receptor and p38 MAPK-mediated pathway. Biochem. Biophys. Res. Commun., 339 (2), 562-568.

Chun, Y.J., Kim, M.Y. and Guengerich, F.P., 1999. Resveratrol is a selective human cytochrome P450 1A1 inhibitor. Biochem. Biophys. Res. Commun., 262(1), 20-24.

Ciolino, H.P. and Yeh, G.C., 1999. Inhibition of aryl-hydrocarbon-induced cytochrome P-450 1A1 enzyme activity and CYP1A1 expression by resveratrol. Mol. Pharmacol. 56, 760-767.

Emoto, C., Murase, S., Sawada, Y. and Iwasaki, K.., 2005. In vitro inhibitory effect of 1-aminobenzotriazole on drug oxidations in human liver microsomes: a comparison with SKF-525A. Drug Metab. Pharmacokinet. 20(5), 351-357.

Enya, T. and Suzuki, H., 1997. 3-nitrobenzanthrone, a powerful bacterial mutagen and suspected human carcinogen found in diesel exhaust and airborne particulates. Environ. Sci. Technol. 31, 2772-2776.

Feilberg, A., Ohura, T., Nielsen, T., Poulsen, M.W.B. and Amagai, T., 2002. Occurrence and photostability of 3-nitrobenzanthrone associated with atmospheric particles. Atmos. Environ., 36(22), 3591-3600.

Foster, K.A., Oster, C.G., Mayer, M.M., Avery, M.L. and Audus, K.L., 1998. Characterization of the A549 cell line as a type II pulmonary epithelial cell model for drug metabolism. Exp. Cell. Res., 243, 359-366

Ghio, A.J. and Cohen, M.D., 2005. Disruption of iron homeostasis as a mechanism of biologic effect by ambient air pollution particles. Inhal. Toxicol., 17(13), 709-716.

Hampton, M.B. and Orrenius, S., 1997 Dual regulation of caspase activity by hydrogen peroxide: implications for apoptosis. FEBS Lett., 414, 552-556.

Hansen, T., Blickwede, M. and Borlak, J., 2006. Primary rat alveolar epithelial cells for use in biotransformation and toxicity studies. Toxicol. in Vitro, 20, 757-766

Hemminki, K. and Pershagen, G., 1994. Cancer risk of air pollution: epidemiological evidence. Environ. Health Perspect., 102 (Suppl 4), 187-192.

Hoidal, J.R., 2001. Reactive oxygen species and cell signaling. Am. J. Respir. Cell Mol. Biol., 25, 661-663.

Hukkanen, J., Lassila, A., Paivarinta, K., Valanne, S., Sarpo, S., Hakkola, J., Pelkonen, O. and Raunio, H., 2000. Induction and regulation of xenobiotic-metabolizing cytochrome P450s in the human A549 lung adenocarcinoma cell line. Am. J. Resp. Cell. Mol. Biol., 22, 360-366.

IARC, 1989. Diesel and Gasoline Engine Exhausts and Some Nitroarenes. Monographs on the Evaluation of Carcinogenic Risks to Humans, No. 46. IARC, Lyon.

Karlsson, H.L., Nilsson, L. and Möller, L., 2005. Subway particles are more genotoxic than street particles and induce oxidative stress in cultured human lung cells. Chem. Res. Toxicol., 18(1), 19-23.

Kastan, M.B., Onyekere, O., Sidransky, D., Vogelstein, B. and Craig, R.W., 1991. Participation of p53 protein in the cellular response to DNA damage. Cancer Res., 51, 6304-6311.

Kawanishi, M., Enya, T., Suzuki, H., Takebe, H., Matsui, S. and Yagi, T., 2000. Postlabelling analysis of DNA adducts formed in human hepatoma cells treated with 3-nitrobenzanthrone. Mutat. Res., 470(2): 133-139.

Khan, N., Hadi, N., Afaq, F., Syed, D.N., Kweon, M.-H.. and Mukhtar, H., 2007. Promeganate fruit extract inhibits prosurvival pathways in human A549 lung carcinoma cells and tumor growth in athymic nude mice. Carcinogenesis, 28(1): 163-173.

Kurz, T., Leake, A., VonZglinicki, T. and Brunk, U.T., 2004. Redox-active lysosomal iron is an important mediator of oxidative-stress-induced DNA damage. Biochem. J., 378(Pt 3), 1039-1045

Lau, A.T., He, Q.Y. and Chiu, L.F., 2004. A proteome analysis of the arsenite response in cultured lung cells: evidence for in vitro oxidative stress-induced apoptosis. Biochem. J., 382, 641-650.

LeBel, C.P., Ischiropoulos, H. and Bondy, S.C., 1992. Evaluation of the probe 2',7'-dichlorofluorescein as an indicator of reactive oxygen species formation and oxidative stress. Chem. Res. Toxicol., 5 (2), 227-231.

Lloyd, J.B., Cable, H. and Rice-Evans, C., 1991. Evidence that desferrioxamine cannot enter cells by passive diffusion. Biochem. Pharmacol., 41(9), 1361-1363

Morel, Y., Mermod, N. and Barouki, R., 1999. An autoregulatory loop controllinmg CYP1A1 gene expression: role of H_2O_2 and NF1. Mol. Cell Biology, 19(10), 6825-6832.

Müller, E. and Bayer, O., 1979. Houben-Weyl, Methoden der Organischen Chemie, Bd.7/3c, Anthrachinone, Anthrone, Georg Thieme Verlag, Stuttgart, p 330-332.

Murahashi, T., Watanabe, T., Otake, S., Hattori, Y., Wakabayashi, K. and Hirayama, T., 2003. Determination of 3-nitrobenzanthrone in surface soil by normal-phase high-performance liquid chromatography with fluorescence detection. J. Chromatogr. A 992(1-2), 101-107.

Nagy, E., Johansson, C., Zeisig, M. and Moller, L., 2005. Oxidative stress and DNA damage caused by the urban air pollutant 3-NBA and its isomer 2-NBA in human lung cells analyzed with three independent methods. J. Chromatogr. B Analyt Technol. Biomed. Life Sci., 827(1), 94-103.

Nagy, E., Zeisig, M., Kawamura, K., Hisamatsu, Y., Sugeta, A., Adachi, S. and Möller, L., 2005. DNA adduct formations in rats after intratracheal administration of the urban air pollutant 3-nitrobenzanthrone. Carcinogenesis, 26(10), 1821-1828.

Nagy, E., Adachi, S., Takamura-Enya, T., Zeisig, M. and Moller, L., 2006. DNA damage and acute toxicity caused by the urban air pollutant 3-nitrobenzanthrone in rats: Characterization of DNA adducts in eight different tissues and organs with synthesized standards. Environ. Mol. Mutagen., 47, 541-552.

Nguyen, T., Sherratt, P.J. and Pickett, C.B., 2003. Regulatory mechanisms controlling gene expression mediated by the antioxidant response element. Annu. Rev. Pharmacol. Toxicol., 43, 233-260.

Ovrevik, J., Hetland, R.B., Schins, R.P., Myran, T. and Schwarze, P.E., 2006. Iron release and ROS generation from mineral particles are not related to cytokine release or apoptosis in exposed A549 cells. Toxicol. Lett., 165, 31-38.

Persson, H.L., Nilsson, K.J. and Brunk, U.T., 2001. Novel cellular defense against iron and oxidation: ferritin and autophagocytosis preserve lysosomal stability in airway epithelium. Redox Report, 6(1), 57-63.

Phousongphouang, P.T. and Arey, J., 2003. Sources of the atmospheric contaminants, 2-nitrobenzanthrone and 3-nitrobenzanthrone. Atmos. Environ. 37, 3189-3199.

Rosenkranz, H.S., 1996. Mutagenic nitroarenes, diesel emissions, particulate-induced mutations and cancer: an essay on cancer-causation by a moving target. Mutat. Res. 367(2), 65-72.

Rota, C., Fann, Y.C. and Mason, R.P., 1999. Phenoxyl free radical formation duríng the oxidation of the fluorescent dye 2',7'-dichlorofluorescein by horseradish peroxidase. J. Biol.Chem. 274(40), 28161-28168.

Seidel, A., Dahmann, D., Krekeler, H. and Jacob, J., 2002. Biomonitoring of polycyclic aromatic compounds in the urine of mining workers occupationally exposed to diesel exhaust. Int. J. Hyg. Environ. Health 204(5-6), 333-338.

Shackelford, R.E., Kaufmann, W.K. and Paules, S., 2000. Oxidative stress and cell cycle checkpoint function. Free Radical Biol. Med., 28(9), 1387-1404.

Silverman, D.T., 1998. Is diesel exhaust a human lung carcinogen? Epidemiology, 9, 4-5.

Stiborova, M., Dracinska, H., Hajkova, J., Kaderabkova, P., Frei, E., Schmeiser, H.H., Soucek, P., Phillips, D.H. and Arlt, V.M., 2006. The environmental pollutant and carcinogen 3-nitrobenzanthrone and its human metabolite 3-aminobenzanthrone are potent inducers of rat hepatic cytochromes P450 1A1 and -1A2 and NAD(P)H:quinone oxidoreductase. Drug Metab. Dispos., 34(8), 1398-1405.

Tang, N., Taga, R., Hattori, T., Tamura, K., Toroba, A., Kizu, R. and Hayakawa, K., 2004. Determination of atmospheric nitrobenzanthrones by high-performance liquid chromatography with chemiluminescence detection. Analyt. Sci., 20, 119-123.

Tenopoulou, M., Doulias, P-T., Barbouti, A., Brunk, U. and Galaris, D., 2005. Role of compartmentalized redox-active iron in hydrogen peroxide-induced DNA damage and apoptosis. Biochem. J., 387, 703-710.

Vasiliou, V., Ross, D and Nebert, D.W., 2006. Update of the NAD(P)H:quinone oxidoreductase (NQO) gene family. Hum. Genomics, 2(5), 329-335

Watanabe, T., Hasei, T., Takahashi, Y., Otake, S., Murahashi, T., Takamura, T., Hirayama, T. and Wakabayashi, K., 2003. Mutagenic activity and quantification of nitroarenes in surface soil in the Kinki region of Japan. Mutat. Res. 538(1-2), 121-131.

Watanabe, T., Tomiyama, T., Nishijima, S., Kanda, Y., Murahashi, T. and Hirayama, T., 2005. Evaluation of genotoxicity of 3-amino-, 3-acetylamino- and 3-nitrobenzanthrone using the Ames/Salmonella assay and the Comet assay. J. Health Sci. 51(5), 569-575.

Zhu, H. and Gooderham, N.J., 2006. Mechanisms of induction of cell cycle arrest and cell death by cryptolepine in human lung adenocarcinoma A549 cells. Toxicol. Sci., 91, 132-129.